A Cost-Oriented Control Strategy for Energy Management of a Dual-Mode Locomotive

Chao Jia, Wei Qiao, and Liyan Qu
Power and Energy Systems Laboratory
Department of Electrical and Computer Engineering
University of Nebraska-Lincoln
Lincoln, NE, 68588-0511, USA
cjia@huskers.unl.edu; wqiao3@unl.edu; lqu2@unl.edu

***Abstract*—Energy management plays a significant role in a dual-mode locomotive with multiple power sources. According to the energy cost analysis for different power sources, a cost-oriented control strategy (COCS) is proposed to allocate the power and manage the energy for a dual-mode locomotive with multiple sources, including a DC overhead line, a fuel cell (FC), a battery (BAT), and a supercapacitor (SC). The COCS won the second-place prize in the IEEE Vehicular Technology Society (VTS) Motor Vehicle Challenge 2019 with a total operational cost of 6.06 € for the scoring cycle. Based on the COCS, an improved strategy COCS+ is developed after the challenge to further decrease the global cost. Simulation results show that the COCS+ performs better than the COCS in reducing the DC line electricity costs and the lifetime costs of the FC, BAT, and SC. The global cost is drastically reduced to -4.69 € when using the COCS+.**

Keywords—battery (BAT), dual-model locomotive, energy management strategy (EMS), fuel cell (FC), supercapacitor (SC).

I. INTRODUCTION

The adoption of electrification and hybridization technologies has been proved to be one proactive strategy to reduce pollutant emissions and fuel consumption of on-road vehicles. In recent years, there has been a clear trend towards accelerating the transfer of the electrification and hybridization technologies to off-road vehicles [1]. In hybrid electric and all-electric vehicles, the energy management strategies (EMSs) play a key role to manage the power flows between different energy sources in an efficient way to fulfill the advantages of the electrification and hybridization technologies. This is the primary reason that the IEEE Vehicular Technology Society (VTS) launched the annual Motor Vehicle Challenge (MVC) to promote the development of EMSs for hybrid electric vehicles.

After the success of the first two international MVCs, the third MVC was launched during the 2018 IEEE Vehicle Power and Propulsion Conference (VPPC) in Chicago, IL, USA [2]. The competition is focused on the EMS of a dual-mode locomotive, which can be powered by a non-reversible DC overhead line through a catenary or on-board fuel cell (FC) with a hybrid energy storage system including battery (BAT) and supercapacitor (SC). The participators are required to propose an EMS to reduce the operational costs that consist of hydrogen and electricity costs and increase the lifetime of the on-board energy sources.

Due to several advantages, FC has offered great potential for sustainable transport. FC is an electrochemical energy conversion device that generates electrical energy with heat and water vapor from chemical reactions [3]. Thus, it is a viable option to achieve zero-emission vehicles. The hydrogen tank used in FC systems can be refueled quickly, typically in several minutes [4]. Moreover, FC vehicles (FCVs) outperform battery electric vehicles in terms of driving range. However, FC has some limitations associated with its slow transient response [5]. High dynamical loads and start-stop operations lead to considerable lifetime degradation of FC systems. To meet the load demand with a highly changing power and prolong the lifetime of FC, energy storage devices (ESDs) with fast dynamics, such as BAT and SC, are usually incorporated. Moreover, vehicle kinetic energy can be absorbed by ESDs during the regenerative braking process to reduce the energy consumption. In the last decade, substantial research efforts have been devoted to developing FC-powered locomotives and trams based on combinations of different sources, such as FC-BAT [6]-[8], FC-SC [9], [10], and FC-BAT-SC [11]-[16].

The combination of FC and ESDs further underpins the importance of the EMS. Numerous EMSs for FC-based hybrid locomotives, including rule-based control strategies [6], [8], [9], [11], [16], equivalent consumption minimization strategies [7], [10], [13], predictive control [12], and filtering-based or frequency decoupling control strategy [14], have been reported in the literature. However, none of the locomotives studied in these references is connected to an overhead power line. In this MVC, the dual-mode locomotive can be powered by a DC line and an on-board FC-BAT-SC energy system. The DC line leaves an additional degree of freedom in fulfilling the power requirements of the locomotive, which, however, introduces more challenge to design an advanced EMS.

To distribute the power from different sources economically, it is crucial to compare the corresponding operational costs. In this work, an energy cost (EC) is defined for each power source. Different power sources are ranked according to their ECs. Then, a cost-oriented control strategy

This work was supported in part by the Nebraska Public Power District (NPPD) through the Nebraska Center for Energy Sciences Research (NCESR).

978-1-7281-0962-6/19/$31.00 ©2019 IEEE

(COCS) is proposed. The core rules of the COCS are extracted based on the EC analysis for different power sources. The proposed COCS is a combination of rule-based, filtering-based, and conventional proportional controllers, as well as saturation regulators (SRs) for physical constraints.

Although the COCS achieved good performance in the MVC, it does not fully exploit the EC analysis results. An enhanced strategy COCS+ is designed to split the power with less costs. COCS+ forces the FC to work at the point with the smallest EC and enables the BAT instead of the SC to be responsible for the power range where the BAT's EC is lower. Compared with the COCS, the COCS+ greatly decreases the global cost from 6.06 € to -4.69 €.

The rest of this paper is organized as follows. The locomotive model and operational costs of each power source are described in Section II. Section III presents the EC analysis and the proposed COCS and COCS+. Simulation results are provided and discussed in Section IV. Section V summarizes the work.

II. Model and Cost Descriptions

A. Locomotive Model

Table I lists the parameters and variables of the model. Subscripts in this paper are summarized in Table II. The structural scheme of the dual-mode locomotive is shown in Fig. 1 [2]. It can be powered by a non-reversible DC overhead line through a pantograph or by an on-board polymer electrolyte membrane FC (PEMFC) with a Li-ion BAT and an SC. All of the energy sources are connected to a DC bus [2]. The electrical relationships of the studied locomotive are synthetized in Table III [2]. A MATLAB/Simulink simulation model is built with the Energetic Macroscopic Representation (EMR) [17].

TABLE I. Model Parameters and Variables

Symbol	Variables	Units
A	current	A
E	energy	kWh
J	current density	A/cm²
$\dot{m}$	mass flow	g/s
N_{start}	start number of FC	-
p	power	W
Q	capacity	Ah
R	resistor	Ω
V	voltage	V
t_{use}	use time	h
α	load coefficient of the FC degradation function	-
Δ	degradation degree	-
δ_0	load coefficient of the FC degradation function	-
η	efficiency	-
FC_{cost}	FC cost of per unit of power	€/kW
SC_{cost}	SC cost per unit of energy	€/kWh
B_{cost}	BAT cost per unit of energy	€/kWh
N_{cost}	cost of the electricity network per unit of energy	€/MWh
S	ON-OFF State	-
S_{cell}	active surface of a fuel cell	cm²

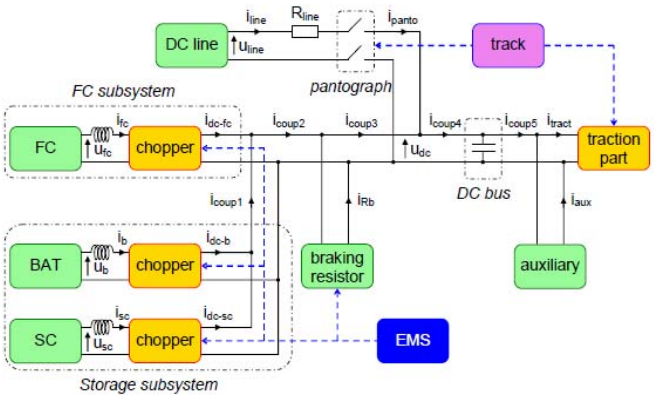

Fig. 1. Block diagram of the dual-mode locomotive.

TABLE II. Subscripts

Symbol	Meaning	Symbol	Meaning
b , B	battery	avg	average value
fc , FC	fuel cell	cmd	command value
H_2	hydrogen	$meas$	measure value
net	electricity network	max	maximum value
sc , SC	supercapacitor	min	minimum value
Rb	brake resistor	rat	rate value
$sust$	charge sustaining	ref	reference value
dc	boost chopper	tot	total value
$panto$	pantograph	$line$	DC line

TABLE III. Electrical Relationships of the Studied Locomotive

BAT and SC boost chopper	$i_x = \frac{u_{dc} i_{dc-x}}{\eta_{dc-x}^{\gamma} u_x}$ $with\ X \epsilon [b, sc]$, $\begin{cases} i_{dc-x} = i_{dc-x-ref}; \\ u_{dc} > u_x \end{cases}$ $i_{x-min} \le i_x \le i_{x-max}$; $and\ \begin{cases} \gamma = 1\ if\ u_{dc} i_{dc-x} \ge 0 \\ \gamma = -1\ if\ u_{dc} i_{dc-x} < 0 \end{cases}$;	(1)
FC boost chooper	$i_{fc} = \frac{u_{dc} i_{dc-fc}}{\eta_{dc-fc} u_{fc}}\ with\ \begin{cases} i_{dc-fc} = i_{dc-fc-ref}; \\ u_{dc} > u_{fc} \end{cases}$ $and\ \begin{cases} 0 \le i_{fc} \le i_{fc-max} \\ A_{min} \le \frac{d}{dt} i_{fc} \le A_{max} \end{cases}$;	(2)
DC line and pantograph	$\begin{cases} \text{Pantograph connect (ON)} \\ i_{line} = i_{panto} = \frac{u_{line} - u_{dc}}{R_{line}} \ge 0 \end{cases}$	(3)
	$\begin{cases} \text{Pantograph disconnect (OFF)} \\ i_{line} = i_{panto} = 0 \end{cases}$	(4)
Braking resistor	$i_{Rb} = i_{Rb-ref}\ with\ i_{Rb} \ge 0$	(5)
DC bus	$i_{coup4} - i_{coup5} = C_{dc} \frac{d}{dt} u_{dc}$	(6)
Current nodes	$i_{coup1} = i_{dc-b} + i_{dc-sc}$	(7)
	$i_{coup2} = i_{coup1} + i_{dc-fc}$	(8)
	$i_{coup3} = i_{coup2} + i_{Rb}$	(9)
	$i_{coup4} = i_{coup3} + i_{panto}$	(10)
	$i_{coup5} = i_{tract} + i_{aux}$	(11)

Mathematical models of the FC, BAT, and SC are briefly resumed for the purpose of the EMS design. The FC model is defined by the polarization curve: the voltage of one cell is a function of the current density. Then, the FC output power can be derived as a function of current shown in (12) and Fig. 2.

$$\begin{cases} V_{fc-cell} = f\left(J_{fc-cell}\right) \\ J_{fc-cell} = i_{fc} / S_{cell} \end{cases} \Rightarrow V_{fc-cell} = f\left(i_{fc}\right) \Rightarrow P_{fc} = f\left(i_{fc}\right) \quad (12)$$

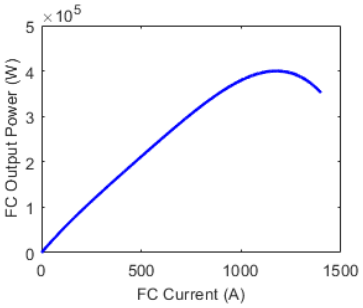

Fig. 2. FC output power versus current.

The BAT is modelled by using the open-circuit voltage and a series resistor. Both parameters are indexed with the State of Charge (SoC). The SC is modelled based on an equivalent circuit model named Zubieta-Bonert model [18], which is composed of two RC branches.

B. Operational Costs

When the locomotive is operated to follow the speed profile, the current required for traction and auxiliary subsystems is imposed on the DC bus. As shown in Fig. 1, the EMS is responsible for managing four different power sources to meet the demand currents. Moreover, the proposed EMS is expected to minimize the energy consumption, such as electricity and hydrogen, and increase the lifetime of the FC, BAT, and SC. At the same time, the physical constraints on the FC, BAT, SC, boost choppers, and DC bus should be satisfied over the whole speed profile. In this challenge, a unified approach is adopted to measure the operational costs of different power sources, which are defined in (13)-(23), where $€_{net}$ is the cost of the electricity from the DC line; $€_{H_2}$ is the hydrogen cost; $€_{fc}$, $€_{sc}$, and $€_b$ represent the lifetime degradation costs of the FC, SC, and BAT, respectively.

$$€_{tot}(t) = €_{net}(t) + €_{H_2}(t) + €_{fc}(t) + €_{sc}(t) + €_b(t) + €_{sust}(t) \quad (13)$$

$$€_{net}(t) = \frac{N_{cost}}{3600 * 10^6} \int_0^t p_{line}(t) dt \quad (14)$$

$$€_{H_2}(t) = \frac{H_{2\text{-}cost}}{10^3} \int_0^t \dot{m}_{H_2}(t) dt \quad (15)$$

$$€_{fc}(t) = P_{fc\text{-}rat} \bullet FC_{cost} \Delta_{fc}(t) / 10^3 \quad (16)$$

$$\Delta_{fc}(t) = N_{start} \Delta_{start}(t) + \int_0^t \delta(t) dt \quad (17)$$

$$\delta(t) = \frac{\delta_0}{3600} \left(1 + \frac{\alpha}{P_{fc-rat}^2} \left(p_{fc}(t) - p_{fc-rat}\right)^2\right) \quad (18)$$

$$€_{sc}(t) = E_{sc-rat} SC_{\text{cost}} \Delta_{sc}(t) \quad (19)$$

$$\Delta_{sc}(t) = t_{use} / \left(30 * 10^3\right) \quad (20)$$

$$€_b(t) = E_{b-rat} B_{cost} \Delta_b(t) \quad (21)$$

$$\Delta_b(t) = \frac{1}{3600 * 15 * 10^3 * Q_{b-rat}} \int_0^t \left| f\left(SoC_b\right) * g\left(i_b\right) * i_b(t) \right| dt \quad (22)$$

$$€_{sust}(\mathrm{t}) = \frac{N_{cost}}{10^3} \left(\eta_{dc-b-avg} * E_{b-end} + \eta_{dc-sc-avg} * E_{sc-end}\right) \quad (23)$$

Since the final SoC of the BAT and SC may be different for each participant's real-time EMS, a charging sustaining cost $€_{sust}$ is used to sustain the SoC. Negative and positive penalties mean that the BAT and SC have been charged and discharged, respectively.

C. Costs Reformulation

It will be more convenient to define the total operational cost of each energy source as follows.

$$€_{FC} = €_{fc} + €_{H_2} \quad (24)$$

$$€_B = €_b + \frac{N_{cost}}{10^3} \eta_{dc-b-avg} * E_{b-end} \quad (25)$$

$$€_{SC} = €_{sc} + \frac{N_{cost}}{10^3} \eta_{dc-sc-avg} * E_{sc-end} \quad (26)$$

Thus, the total cost is transformed as

$$€_{tot}(\mathrm{t}) = €_{net}(\mathrm{t}) + €_{FC}(\mathrm{t}) + €_{SC}(\mathrm{t}) + €_B(\mathrm{t}) \quad (27)$$

Since the "always-on" strategy is adopted for the FC, the $€_{FC}$ in (24) does not take the start-stop degradation into account. This will be explained in the next section.

III. Cost Analysis and EMS Design

A. Energy Costs

To split the power economically among different energy sources, it is critical to analyze and compare the operational costs incurred by each energy source. Through a comprehensive analysis of the energy source models and operational cost equations (14)-(26), the *EC* of each energy source is defined as following for a fair ranking of different energy sources.

$$EC_x = \begin{cases} \dfrac{€_x(p_{x-dc})}{|p_{x-dc}|} & if\ p_{x-dc} \neq 0 \\ 0 & if\ p_{x-dc} = 0 \end{cases} \quad x \in [B, FC, net, SC], \quad (28)$$

where p_{x-dc} represents the power flowing into or drawn from the DC bus.

The efficiency of the boost choppers is considered for the power transfer between the energy sources and the DC bus. According to (28), EC_x can be directly derived as a function of p_{x-dc} for $x \in [FC, net, SC]$. The p_{B-dc} depends on both the BAT current and SoC, so does the EC_B.

According to the EC_x values of different energy sources plotted in Fig. 3 and Fig. 4, the following results can be obtained.

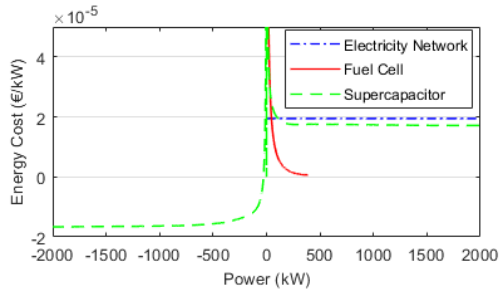

Fig. 3. Energy costs of the electricity network, FC, and SC.

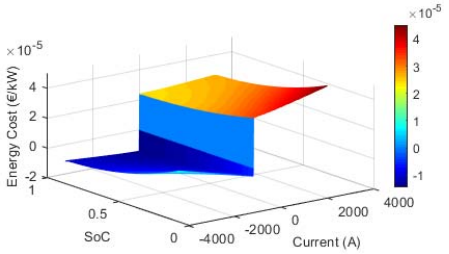

Fig. 4. Energy cost of the BAT.

1) If $p_{x-dc} > 0$, the ranking $EC_{fc} < EC_{sc} < EC_{net} < EC_b$ is true except for the condition when p_{x-dc} is very low.

2) If $p_{x-dc} < 0$, $EC_{sc} < EC_b$ is guaranteed except for the small range where p_{x-dc} is close to zero.

B. Cost-Oriented Control Strategy (COCS)

1) FC Current Control

One drawback of the FC is slow startup. The start-stop process also leads to a significant operational cost that is illustrated in (17). To avoid these problems an "always on" strategy is applied to the FC [6], [7]. Once the FC starts, it will be kept to work continuously until the entire trip ends. Based on the *EC* analysis, the FC provides the power with a lower operational cost. The most economical operating point is at the rated power p_{fc-rat} with the rated current. Thus, the FC is controlled by the DC-DC chopper to work at this point as much as possible.

Rule 1. If the locomotive starts with the condition that the DC overhead line is available, the FC remains off until the DC line becomes unavailable.

Rule 2. After the FC starts, the output current is regulated according to the SoC_b. When the SoC_b is smaller than the reference value, the FC outputs the rated current all the time. When the SoC_b is over the reference value, the output current is linearly decreased with the excess.

There are several constraints on the FC and its dc-dc like the maximum power of dc-dc, and the maximum current and current variation rate of FC. An SR is designed to satisfy these constraints, as shown in Fig. 5.

2) SC Current Control

According to the *EC* analysis, the SC outperforms the BAT in a large power range. Thus, it is preferable to use the SC to provide or absorb power. A filter-based controller is designed to allocate the output current of the SC, which is responsible for the high frequency components of $i_{coup2-ref}$.

Rule 3. During the regenerative mode, charge the SC firstly.

Rule 4. During the traction mode, the SC is charged to SoC_{sc-ref} with a proportional controller ($Ctrl_p$) when the DC line is available. If the DC line is not available, the filter-based controller ($Ctrl_f$) is used to charge and discharge the SC.

Then, the value of $i_{dc-sc-ref}$ is managed by the SR to satisfy the constraints on the maximum power of the chopper as well as the output voltage and current of the SC.

3) BAT Current Control

After the output currents of the FC and SC are decided, it is simple to obtain the required current of the BAT.

Rule 5. If the DC line is active and SOC_b is less than the reference value, the BAT is charged with a larger current. Since the charging current is negative, the *min* function is used in (31).

Rule 6. If the DC line is unavailable and SOC_b is not less than the reference value, the BAT is charged.

Similar to the SC, an SR is used to limit $i_{dc-b-ref}$ under the constraints of the BAT and the chopper.

According to the above analysis and combining the current control loops described above, the complete COCS is obtained, as illustrated in Fig. 6.

C. Enhanced Strategy COCS+

According to Fig. 3 and 4, the FC has the least EC among all of the power sources when the power sources are providing power. Therefore, the FC should be started as the trip begins and kept working at the rated power, which is different from *Rule 1* and *Rule 2*.

Besides, it is worth noting that EC_{sc} is not continuous at the point of zero power, which is a local minimum. As mentioned above, $EC_{sc} < EC_b$ cannot be guaranteed in the small range near zero power. Thus, if the required power of the SC is located in this range, the SC does not operate. Due to less costs, the BAT is assigned to absorb or provide power. Both the filter-based controller and the proportional controller can be avoided. The current commands for the FC, SC, and BAT are calculated with (32)-(34). The COCS+ can be implemented by replacing (29)-(31) with (32)-(34), respectively.

IV. Simulation Results

The proposed COCS is tested with three driving cycles that are provided by the MVC. Every cycle consists of a speed profile, DC line ON-OFF states, and an auxiliary current profile. Fig. 7 shows the speed profile and ON-OFF states of each cycle. Participants are ranked on the basis of the cost function with an unknown scoring driving cycle [2].

$$i_{dc-fc-ref}=\begin{cases}0, & if\ S_{line}=ON\ and\ S_{fc}=OFF\\ i_{dc-fc-rat}, & if\ SoC_b<SoC_{b-ref}\\ (1-SoC_b)*i_{dc-fc-rat}/gain & if\ SoC_b\geq SoC_{b-ref}\end{cases} \tag{29}$$

$$i_{dc-sc-ref}=\begin{cases}i_{coup2-ref}, & if\ i_{coup5-meas}<0\\ Ctrl_f(i_{coup2-ref}), & if\ i_{coup5-meas}>0\ and\ S_{line}=OFF\\ Ctrl_p(SoC_{sc}), & if\ i_{coup5-meas}>0\ and\ S_{line}=ON\end{cases} \tag{30}$$

$$i_{dc-b-ref}=\begin{cases}i_{coup2-ref}-i_{dc-sc-sat} & if\ S_{line}=OFF\\ min(i_{coup2-ref}-i_{dc-sc-sat},i_{dc-b-charge-ref}) & if\ SOC_b\leq SoC_{b-ref}\ and\ S_{line}=ON\end{cases} \tag{31}$$

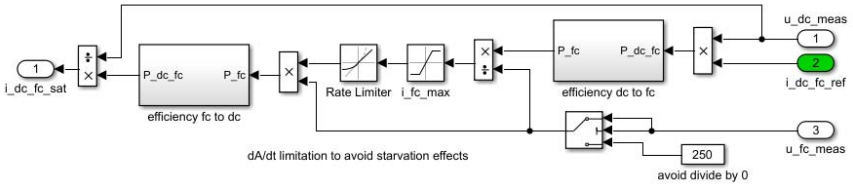

Fig. 5. The SR for output current of FC's chopper

$$i_{dc-fc-ref}=i_{dc-fc-rat} \tag{32}$$

$$i_{dc-sc-ref}=\begin{cases}0 & if\ i_{coup2-ref}\geq 0\ and\ S_{line}=ON\\ \frac{i_{dc-sc-min}*u_{sc-meas}}{u_{dc-meas}} & if\ i_{coup2-ref}<0\ and\ SoC_{sc}<SoC_{sc-ref}\\ i_{coup2-ref} & else\end{cases} \tag{33}$$

$$i_{dc-b-ref}=\begin{cases}i_{coup1-ref} & if\ i_{coup1-ref}\geq 0\ and\ S_{line}=OFF\\ \frac{i_{dc-b-min}*u_{b-meas}}{u_{dc-meas}} & if\ i_{coup1-ref}<0\ and\ SoC_b<SoC_{b-ref}\\ 0 & else\end{cases} \tag{34}$$

The operational costs of the three cycles are listed in Table IV. The value of $€_{fc}$ is related to the amount of the used time of the FC. The result indicates that the SC is kept working during the entire cycle. The SC current control in the COCS fails to reduce the lifetime cost of the SC. In addition, a significant amount of electric power drawn from the DC line is used to charge the BAT and the SC in the COCS. However, according to EC plots, it is more economic to charge the BAT and SC with the FC power rather than the electric power from the DC line. Finally, the power variations of the FC add extra costs. These drawbacks above can be overcome by using the COCS+. Compared with the COCS, $€_{net}$ and $€_{sc}$ are decreased greatly when using the COCS+, as shown in Table IV.

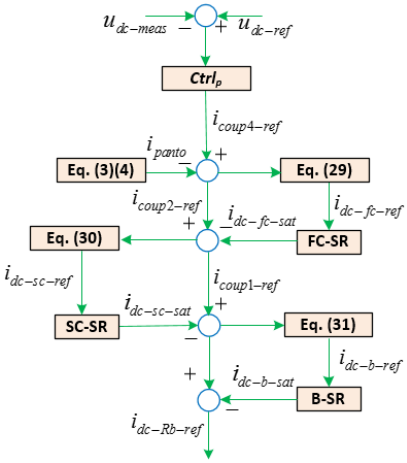

Fig. 6. Flow chart of the proposed COCS.

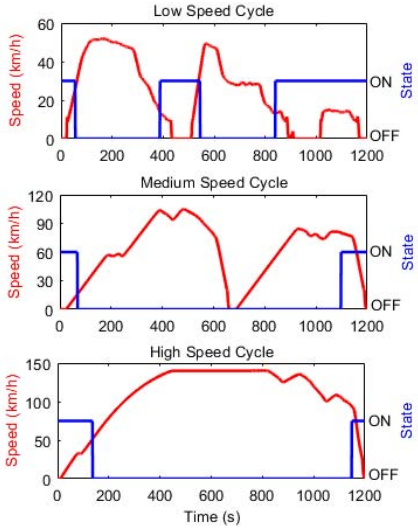

Fig. 7. Speed profile (red) and DC line ON-OFF states (blue).

TABLE IV. OPERATIONAL COSTS OF THE LOCOMOTIVE

Cycle	EMS	$€_{net}$	$€_{H_2}$	$€_{fc}$	$€_{sc}$	$€_b$	$€_{sust}$	$€_{tot}$
Low Speed Cycle	COCS	2.94	0.08	4.27	0.62	2.38	-7.39	2.90
	COCS+	0.03	0.08	4.27	0.04	1.24	-4.10	1.57
Medium Speed Cycle	COCS	1.11	0.08	4.26	0.62	1.60	-2.71	4.97
	COCS+	0.00	0.08	4.27	0.23	1.38	-1.23	4.73
High Speed Cycle	COCS	1.91	0.07	4.25	0.62	3.38	4.20	14.53
	COCS+	0.05	0.08	4.27	0.15	3.10	5.62	13.28
Scoring Cycle	COCS	6.15	0.32	7.09	3.90	6.77	-18.17	6.06
	COCS+	0.45	0.53	5.75	0.30	5.98	-17.70	-4.69

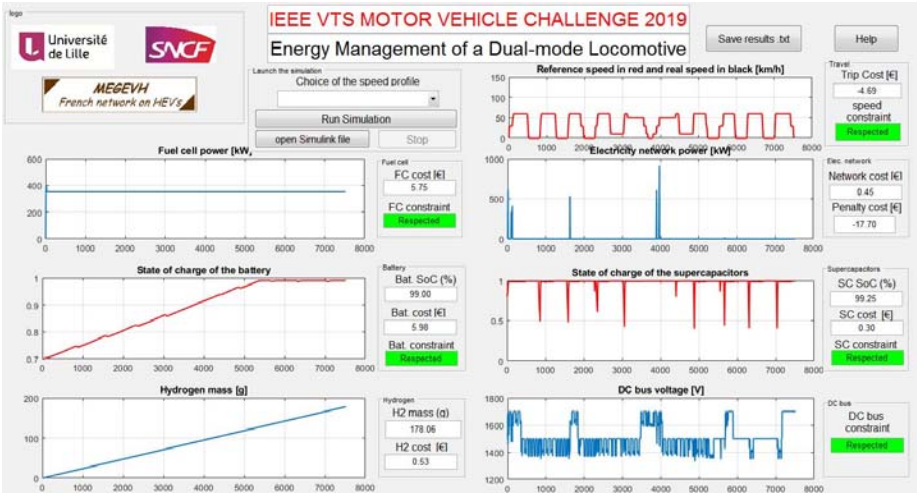

Fig. 8. Simulation results of the COCS+.

The COCS and COCS+ are tested with the scoring cycle by the MVC committee and the authors, respectively. The operational costs are presented in Table IV. Moreover, the results of using the COCS+ are also illustrated in Fig. 8, which shows the operation profiles of different power sources.

V. Conclusions

Based on the comparison of the ECs of four different power sources, a heuristic COCS was proposed for the energy management of a dual-mode locomotive. The COCS regulates the current commands of the FC, SC, BAT, and braking resistor to reduce the total operational cost of the locomotive and satisty the power demands and physical constraints.

The proposed COCS won the second place in the IEEE VTS MVC 2019 with a total operational cost of 6.06 € for the scoring cycle. The total cost of the first-place winner is 6.03 €. Based on the COCS, an improved EMS COCS+ was developed after the challenge to further decrease the global cost to -4.69 €.

References

[1] C. Jia, W. Qiao, and L. Qu, "Modeling and control of hybrid electric vehicles: a case study for agricultural tractors," in *Proc. IEEE Vehicle Power and Propulsion Conf.,* Aug. 2018, pp. 1-6.

[2] W. Lhomme, *et al.*, "IEEE VTS Motor vehicles Challenge 2019 – Energy management of a dual-model locomotive," in *Proc. IEEE Vehicle Power and Propulsion Conf.,* Aug. 2018, pp. 1-6.

[3] J. Kim and S. Kim, "Obstacles to the success of fuel-cell electric vehicles: are they truly impossible to overcome?" *IEEE Electrification Magazine*, vol. 6, no. 1, pp. 48-54, Mar. 2018.

[4] G. J. Offer, D. Howey, M. Contestabile, R. Clague and N. P. Brandon, "Comparative analysis of battery electric, hydrogen fuel cell and hybrid vehicles in a future sustainable road transport system," *Energy Policy*, vol. 38, pp. 24-29, Sep. 2010.

[5] M. Carignano, V. Roda, R. Costa-Castello, L. Valino, A. Lozano and F. Barreras, "Assessment of energy management in a fuel cell/battery hybrid vehicle," *IEEE Access*, vol. 7, pp. 16110-16122, 2019.

[6] P. Garcia, L. M. Fernandez, C. A. Garcia, and F. Jurado, "Energy management system of fuel-cell-battery hybrid tramway," *IEEE Trans. Ind. Electron*, vol. 57, no. 12, pp. 4013-4023, Dec. 2010.

[7] J. P. Torreglosa, F, Jurado, P. Garcia, and L. M. Fernandez, "Hybrid fuel cell and battery tramway control based on an equivalent consumption minimization strategy," *Control Eng. Pract*., vol. 19, pp. 1182-1194, 2011.

[8] Y. Han, X. Meng, G. Zhang and Q. Li, "An energy management system based on hierarchical control and state machine for the PEMFC-battery hybrid tramway," *in Proc. IEEE Transportation Electrification Conf. and Expo, Asia-Pacific*, Aug. 2017, pp. 1-5,.

[9] Y. Han, Q. Li, T. Wang, W. Chen and L. Ma "Multisource coordination energy management strategy based on SOC consensun for a PEMFC-battery-supercapacitor hybrid tramway," *IEEE Trans. Veh. Technol*., vol. 67, no. 1, pp. 296-305, Jan. 2018.

[10] Y. Yan, Q. Li, W. Chen, B. Su, J. Liu and L. Ma, "Optimal energy management and control in multimode equivalent energy consumption of fuel cell/supercapacitor of hybrid electric tram*,"IEEE Trans. Ind. Electron*., vol. 66, no. 8, pp. 6065-6076, Aug. 2019.

[11] Z. Hong, Y. Han, Q. Li, and W. Chen, "Design of energy management system for fuel cell/supercapacitor hybrid locomotive," *in Proc. IEEE Vehicle Power and Propulsion Conf*eren, Dec. 2016, pp. 1-5.

[12] J. P. Torreglosa, P. Garcia, L. F. Fernandez, and F. Jurado, "Predictive control for the energy management of a fuel-cell-battery-supercapacitor tramway," *IEEE Trans. Ind. Inf.*, vol. 10, no. 1, pp. 276-285, Feb. 2014.

[13] P. Garcia, J. P. Torreglosa, L. M. Fernandez, and F. Jurado, "Viability study of a FC-battery-SC trammway controlled by equivalent consumption minimization strategy," *Int. J. Hydrogen Energy*, vol. 37, no. 11, pp. 9368-9382, Jun. 2012.

[14] Q. Li, W. Chen, Z. Liu, M. Li and L. Ma, "Development of energy management system based on a power sharing strategy for a fuel cell-battery-supercapacitor hybrid tramway," *J. Power Sources*, vol. 279, pp. 267-280, Dec. 2015.

[15] Q. Li, T. Wang, C. Dai, W. Chen and L. Ma. "Power management strategy based on adaptive droop control for a fuel cell-battery-supercapacitor hybrid tramway," *IEEE Trans. Veh. Technol.*, vol. 67, no. 7, pp. 5658-5670, July 2018.

[16] K. Yedavlli, L. Guo, and D. S. Zinger, "Simple control system for a switcher locomotive hybrid fuel cell power system," *IEEE Trans. Ind. Appl.*, vol. 47, no. 6, pp. 2384-2394

[17] A. Bouscayrol, B. Davat and B. de Fornel, "Control structures for multi-machine multiconverter systems with upstream coupling", *Mathematics and Computer in Simulation*, vol. 63, no. 3-5, pp. 261-270, Nov. 2003.

[18] L. Zubieta and R. Bonert, "Characterization of double-layer capacitors for power electronics applications," *IEEE Trans. Ind. Appl*., vol. 36, no. 1, pp. 199-205, Jan./Feb. 2000.